

# Enhanced annealing kinetics in ion-implanted $\text{In}_x\text{Al}_{1-x}\text{As}$ studied by x-ray diffractometry

Roy Clarke,<sup>a)</sup> Waldemar Dos Passos,<sup>a)</sup> Yi-Jen Chan, and Dimitris Pavlidis  
Center for High Frequency Microelectronics, Department of Electrical Engineering and Computer Science,  
The University of Michigan, Ann Arbor, Michigan 48109-2122

(Received 30 November 1990; accepted for publication 19 February 1991)

We report a rapid thermal annealing (RTA) enhancement of the structural coherence of Si-implanted  $\text{In}_x\text{Al}_{1-x}\text{As}$  ( $x \approx 0.54$ ) layers on (100)InP. Under these annealing conditions (750 °C for 30 s), the enhancement occurs only in implanted samples and is characterized by the appearance of pendellösung fringes in double-crystal x-ray diffraction. Measurements of the parallel ( $\epsilon_{\parallel}$ ) and perpendicular ( $\epsilon_{\perp}$ ) lattice mismatch show a slight relaxation in  $\epsilon_{\perp}$  during RTA without significant generation of dislocations ( $\epsilon_{\parallel} = 0$ ). The results suggest an electronic mechanism for the increased efficiency of RTA in implanted samples.

$\text{In}_x\text{Al}_{1-x}\text{As}/\text{In}_x\text{Ga}_{1-x}\text{As}$  high electron mobility transistors (HEMTs) and heterostructure insulated gate FETs (HIGFETs) offer new possibilities for high-speed/high-frequency performance of semiconductor devices.<sup>1,2</sup> Ion implantation plays an indispensable role in the realization of such heterostructure devices and heterostructure FET integrated circuits.<sup>3</sup> For example, it is often used in HEMTs to reduce the access resistance to the channel, while for HIGFETs it is used to define the type ( $n$  or  $p$ ) of the FET channel. As an important step in the activation of ion implants, rapid thermal annealing (RTA) has been shown to have several advantages over conventional furnace processing especially for the fabrication of high-speed devices.<sup>4</sup>

In this letter we investigated the effect of ion implantation on the annealing kinetics of  $\text{In}_x\text{Al}_{1-x}\text{As}/\text{InP}$  prototype HIGFET layers, studying the semiconductor material properties by x-ray double-crystal rocking curve analysis.<sup>5</sup> Of particular interest is the quality of the layer structure, especially after a rapid thermal annealing (RTA) treatment used for implant activation. We will show that there are dramatic differences in the structural coherence after RTA depending on whether the layers are virgin or implanted.

For these studies a 5250-Å-thick  $\text{In}_x\text{Al}_{1-x}\text{As}$  ( $x = 0.54$ ), layer<sup>6</sup> was grown by molecular beam epitaxy on a semi-insulating (SI)-InP substrate (see Fig. 1). After growth, Si ions were implanted by a double energy ( $E$ ) process under similar conditions that apply to HIGFET technology, namely  $E_1 = 30$  keV at dose  $D_1 = 2 \times 10^{13}$   $\text{cm}^{-2}$  followed by  $E_2 = 70$  keV,  $D_2 = 4 \times 10^{13}$   $\text{cm}^{-2}$ . RTA capless annealing under Ar gas flow at 750 °C for 30 s was used for implant activation. The material properties before and after RTA were studied by means of double-crystal x-ray diffraction. In this technique the scattered x-ray intensity is measured as a function of rocking angle. A dynamical fit<sup>7</sup> to the intensity profile reveals the amount of strain perpendicular and parallel to the substrate and can be used to probe the degree of structural coherence in the heterostructure. In particular, the interference of x-ray

beams scattered from the InP substrate and from the slightly strained  $\text{In}_x\text{Al}_{1-x}\text{As}$  layer creates a pattern of fringes as the angle of incidence is varied. The amplitude and phase of these fringes (pendellösung) are very sensitive to material parameters such as strain, composition, uniformity, and dislocation density.<sup>8</sup>

Figure 2 compares the rocking curves of the virgin (unimplanted) sample before and after RTA. There is essentially no difference; however, prior to annealing we do observe a slight increase in the splitting between the film peak ( $\omega \approx -545$  arcsec) and the InP(400) substrate peak ( $\omega = 0$ ) on implanted samples. The increase in splitting indicates a small (0.002%) enhancement of the average perpendicular strain as a result of ion implantation.<sup>9</sup> Note that in both curves shown in Fig. 2 the  $\text{In}_x\text{Al}_{1-x}\text{As}$  peak is substantially broader than the substrate peak, which is of instrumental width  $\approx 10$  arcsec. The lower profile in Fig. 2 is a fit using a dynamical scattering model<sup>7</sup> in which the relative lattice spacing of the  $\text{In}_x\text{Al}_{1-x}\text{As}$  layer varies over the range  $\epsilon_{\perp} = 0.37\%$  to  $\epsilon_{\perp} = 0.42\%$ . Here  $\epsilon_{\perp}$  is defined as the percentage mismatch of the overlayer (measured in the perpendicular direction) with respect to the cubic InP substrate. The natural (relaxed) lattice spacing of  $\text{In}_{0.54}\text{Al}_{0.46}\text{As}$  corresponds to  $\epsilon_{\perp}^0 = 0.196\%$ ; a tetragonal distortion<sup>10</sup> of the overlayer accounts for the perpendicular strain,  $\epsilon_{\perp} - \epsilon_{\perp}^0$ .

The small strain nonuniformity present in the as-grown condition is the result of the sluggish kinetics of strained layer molecular beam epitaxy (MBE) growth.<sup>11</sup> The microscopic nature of the strain inhomogeneity is not clear: the  $\text{In}_x\text{Al}_{1-x}\text{As}$  layer at  $x = 0.54$  is certainly well below the critical thickness for dislocation formation

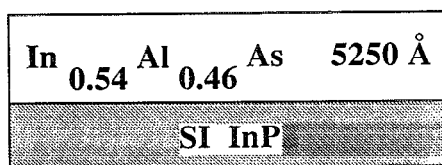


FIG. 1. Schematic layer structure of the  $\text{In}_x\text{Al}_{1-x}\text{As}/\text{InP}$  samples used in this study.

<sup>a)</sup>Also in the Department of Physics.

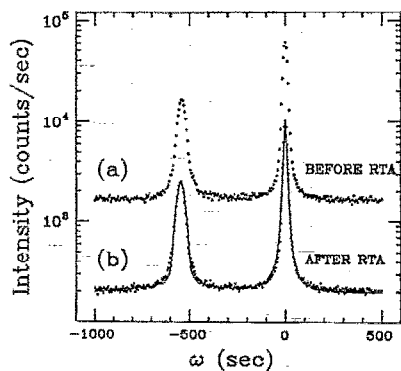


FIG. 2. Typical double-crystal x-ray rocking curves (dots) of the unimplanted sample (a) before and (b) after RTA. The solid line represents a dynamical fit to the x-ray data [see footnote 7]. Note also that the curves (a) and (b) are offset vertically for clarity.

( $x = 0.52$  is lattice matched in InP) and so we expect, and do observe, a coherent pseudomorphic interface with negligible dislocation density. A likely candidate is the presence of steps which may lead to interface roughening in the as-grown state.<sup>12</sup> The sensitivity of the double-crystal technique allows us to measure precisely these subtle departures from perfectly uniform coherent structure.

In Fig. 3 we again compare the x-ray profiles of the sample before and after RTA, this time in the implanted state. An interesting, and (as far as we are aware) previously unobserved, effect occurs: whereas there was virtually no change in the virgin sample, the implanted structure now becomes much more coherent and uniform as the result of an identical RTA treatment. Note the appearance of a well-defined fringe pattern [Fig. 3(b)] which fits almost exactly the calculated profile for the ideal structure shown in Fig. 1 with a uniform pseudomorphic strained overlayer. This finding has been repeated at least three times on three different sets of samples and is quite reproducible.

In addition to the appearance of coherent interference fringes, the values of  $\epsilon_1$  in the implanted samples are also found to relax slightly after RTA. We observe that  $\epsilon_1$  de-

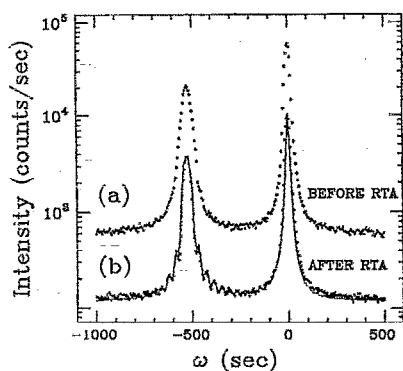


FIG. 3. Typical rocking curves of the implanted sample (a) before and (b) after RTA. Note the distinct formation of the pendellösung fringes only after RTA.

creases from 0.432% to 0.418% while  $\epsilon_{||}$  [measured from (115) rocking curve profiles] remains unchanged at zero within the experimental resolution of 0.001%. These observations provide important clues as to the microscopic consequences of RTA. Firstly, we deduce that the activation barrier<sup>13</sup> for the particular interface defect which gives rise to inhomogeneous strain in the as-grown sample must be quite large (at least 2.5 eV) in the unimplanted sample. This is consistent with interface steps. Secondly, the slight (0.014%) decrease in  $\epsilon_1$  after RTA indicates that ion implantation substantially enhances the kinetics associated with these activation barriers allowing some relaxation of the structure. However, it is important to note that the value of  $\epsilon_1$  after RTA in implanted samples is almost exactly what is expected ( $\epsilon_1 = 0.416\%$ ) for a perfectly pseudomorphic overlayer at this composition (including the tetragonal distortion) and so there is no dislocation formation during RTA.

What then is the mechanism whereby long-range coherence is established in the annealing process when implanted ions are present? We are led to the conclusion that the kinetics of step migration, and concomitant interface smoothing, is influenced strongly by the implants. One possible mechanism might be the local strain fields around the implanted ions. In view of the short penetration range (200–500 Å) of the implanted ions at the energies employed here (30–70 keV), it is unlikely that this mechanism would be very effective in the relatively thick overlayer under consideration. One other possibility is that the coupling efficiency of the RTA light source into the overlayer may be enhanced by the presence of interband states created by implantation.<sup>14</sup> This would lead to enhanced absorption in the infrared region together with increased heating rates and, consequently, more effective annealing of defects. In this way the interface steps could be smoothed without subjecting the sample to prolonged annealing and thus avoiding deterioration of the overlayer stoichiometry.

In summary we have identified a new mechanism whereby the process of rapid thermal annealing appears to be more efficient in ion-implanted samples than in virgin samples. The high sensitivity of x-ray rocking curve analysis facilitates studying the subtle structure changes during thermal processing. The authors wish to acknowledge the support of the Army Research Office (URI program) under contract No. DAAL-03-87-K0007.

<sup>1</sup>G. Ng, D. Pavlidis, M. Jaffe, J. Singh, and H-F. Chau, IEEE Trans. Electron. Device 36, 2249 (1989).

<sup>2</sup>M. D. Feuer, D. M. Tennent, J. M. Kuo, S. C. Shank, B. Tell, and T. Y. Chang, IEEE Electron. Device Lett. 10, 70 (1989).

<sup>3</sup>A. I. Akinwande, IEEE IEDM Tech. Dig. 97 (1989).

<sup>4</sup>P. Pearah, T. Henderson, J. Klem, H. Morkoc, B. Nilsson, O. Wu, A. W. Swanson, and D. R. Chen, J. Appl. Phys. 56, 1851 (1984).

<sup>5</sup>M. H. Lyons and M. A. G. Halliwell, Inst. Phys. Conf. Ser. 76, 445 (1985).

<sup>6</sup>The  $\text{In}_{0.48}\text{Al}_{0.52}$  As layer was lightly doped with Si during growth. This bulk doping ( $\approx 5 \times 10^{17} \text{ cm}^{-3}$ ) is approximately  $\frac{1}{50}$  of the ion-implanted dopant density.

<sup>7</sup>M. J. Hill and B. K. Tanner, J. Appl. Cryst. 18, 446 (1985).

<sup>8</sup>L. Tapfer and K. Ploog, Phys. Rev. B 33, 5565 (1986).

- <sup>9</sup>B. M. Paine, N. N. Hurvitz, and V. S. Speriosu, *J. Appl. Phys.* **61**, 1335 (1987).
- <sup>10</sup>J. Hornstra and W. J. Bartels, *J. Cryst. Growth* **44**, 513 (1978).
- <sup>11</sup>K. H. Chang, P. R. Berger, R. Gibala, P. K. Bhattacharya, J. Singh, J. F. Mansfield, and R. Clarke, in *Dislocations and Interfaces in Semiconductors*, edited by K. Rajan, J. Narayan, and D. Ast (Metallurgical Society, Warrendale, PA, 1988), p. 157.
- <sup>12</sup>J. Singh and K. K. Bajaj, *J. Vac. Sci. Technol. A* **6**, 2022 (1988).
- <sup>13</sup>J. M. Bonar, R. Hull, R. J. Malik, R. W. Ryan, and J. F. Walker, *Proc. Mater. Res. Soc.* **160**, 117 (1990).
- <sup>14</sup>W. O. Adekoya, M. Hage-Ali, J. C. Muller, and P. Siffert, *J. Appl. Phys.* **64**, 666 (1988).